Supporting Information

Gade et al. 10.1073/pnas.1119273109

SI Materials and Methods

Cell Lines, Plasmids, Antibodies, and Other Reagents. Although two proteins ATF6α and ATF6β originating from different genes are known, the current studies used ATF6α (referred to as ATF6) because it is a known positive regulator of ER stress (1). Isogenic pairs of MEFs from wild-type and mice lacking individual genes for C/EBP-β and ATF6 (2) were used in these studies. Human or mouse IFN-γ (PBL Biomedical Labs) was used at 500 U/mL for 16 h unless indicated otherwise. Full-length HA-tagged ATF6 (HA-ATF6) (3), Flag-ATF6, and protease-resistant ATF6 mutant (HA-ATF6mut) lacking the S1P cleavage site (4), Golgi marker (galactosyl transferase fused to red fluorescent protein; DS1-GT) (5), were described earlier. All these constructs have an N-terminal tag. All other ATF expression vectors were kindly provided by Tsonwin Hai (Ohio State University, Columbus, OH) and Gerald Theil, (University of the Saarland Medical Center, Homburg, Germany). *Dapk1-Luc* and *Dapk1 CRE/ATF mut-Luc* were described earlier (6). Expression vectors for wild-type C/EBP-β (LAP2 isoform) and its mutants (Mut1, Mut2, $T^{189}A$, and $T^{189}D$) and ERK1/2-depleted MEFs were described earlier (6). GFP-LC3 expression vector was from Beth Levine (University of Texas Southwestern Medical Center, Dallas, TX). Rabbit antibodies against ATF6 and C/EBP-β (Santa Cruz Biotechnology), mouse monoclonal ATF6 antibody that detects full length and cleaved form (Imgenex), FITC-conjugated anti-mouse IgG (Invitrogen), rabbit antibodies against actin, BiP and mouse monoclonal antibodies against DAPK1 (Sigma-Aldrich), GM130 (BD Pharmingen) FLAG-epitope, HA-epitope, and LC3 (Cell Signaling) were used in these studies. The rabbit antibodies against ATF6 do not detect the cleaved from of ATF6. The 3-methyl adenine (3-MA, an inhibitor of autophagy) and chloroquine (inhibitor of fusion of autophagosome and lysosomes) were from Sigma-Aldrich. DNA transfection was performed as described in our earlier studies (6). All DNA transfection studies were performed with transgene expression levels corresponding to that of endogenous levels to avoid potential overexpression artifacts. Lentiviral vectors carrying short hairpin RNAs (shRNAs) specific for human and mouse ATF6 were purchased from Open Biosystems. Viral particles were prepared and used as described in our earlier studies (6). Depletion of the target gene product was assessed by performing Western blot analyses of total cell extracts. shRNA sequence details are below.

Bacterial Infection. Experiments were performed by using 6- to 8-wk-old *WT* and $Atf6^{-/-}$ mice (2) with the C57/BL6 background. Mice were housed at the University of Maryland, Baltimore animal facility according to Institutional Animal Care and Use Committee-approved protocols. For survival studies, mice ($n = 7$ per group) were injected i.p. with 1×10^6 *Bacillus anthracis* Sterne 34F2 spores and observed for morbidity or mortality up to 9 d after infection (7). In separate experiments, spleen and liver were harvested from *WT* and $Atf6^{-/-}$ mice at 96 h after infection for bacterial load analysis. Peritoneal macrophages were collected from these mice, plated on to chamber slides (Labtek), and fixed after 6 h. The slides were to score for the differences in LC3 puncta formation by using immunofluorescence.

Reporter Gene Assays. Reporter gene assays were performed as described (6). Luciferase activity was determined after indicated treatments and normalized to that of β-galactosidase. Each experiment was repeated at least three times, and triplicates were used for each sample.

Western Blot, Immunoprecipitation, ChIP Assays, re-ChIP Assays, Real-Time PCR (qPCR). Western blot and immunoprecipitation analyses with the indicated antibodies were performed as described earlier (6). Standard ChIP assays were performed, and the ChIPed DNA was used for normal or real-time PCR as described in our previous studies (6). In re-ChIP experiments, after immunoprecipitating the chromatin with first antibody, protein–DNA complexes were eluted from the protein G magnetic beads. The chromatin from the first ChIP reaction was dissociated by using a high salt buffer, and then chromatin was desalted by using a column supplied with a commercially available Re-ChIP kit (Active Motif). The desalted sample was diluted 10-fold with the Re-ChIP buffer and used for a second round of ChIP with 2° antibody before reverse- cross-linking and recovery of DNA (8). DNA from the second round ChIP was PCR amplified as described in our previous studies (5). DNA recovered from the ChIP and re-ChIP reactions was subjected to qPCR analysis for quantifying the differences between various samples. Six independent samples were quantified per condition. Real-time PCR analysis was performed by using gene-specific primers as described in our earlier studies (6). The mRNA for ribosomal protein L32 (Rpl32) was used as an internal control. Triplicate reactions were performed for each sample, and each experiment was repeated three times with independent batches of RNA. Statistical significance of the differences was determined by using the Student t test, where $P < 0.05$ was considered significant.

Lentiviral shRNAs. Mouse and human ATF6-specific shRNAs (nucleotides in boldface type) have the following sequences: 5′CCGG**GCCATCATCA TTCAGA CACTAC**TCGA**G TAGTGT-CTGAATGATGATGGC**TTTTT3′, and 5′CCGG**GCAGCAACC-AATTATCAGTTT**CTCGAG**AAACTGATAATTGGTTGCTC**TT-TTT3′, respectively. All these shRNAs target the coding region in the specific mRNAs in their respective species. Because their target sequences are not identical, these shRNAs could not direct the degradation of the endogenous mRNAs when infected in cells of another species. In addition, in some experiments, we used scrambled shRNA as controls.

FRET Constructs and Primer Sequences. ATF6 primers: Fwd 5′ GCC AAG CTT TT GCC ACC ATG GGG GAG CCG GCT GGG G 3′ and Rev 5′GAA GGG CCC CC TTG TAA TGA CTC AGG GAT G3′; C/EBP-β primers: Fwd 5′ GCC AAG CTT TT GCC ACC ATG GAA GTG GCC AAC TTC TAC and Rev 5′GAA GGG CCC CC GCA GTG ACC CGC CGA GGC 3′.

FRET Analysis. ATF6 and C/EBP-β ORFs were subcloned, after PCR, into HindIII and ApaI sites of mVenus-C1 (9) and mCerulean-C1 (10) vectors, respectively (see above). $Cebpb^{-/-}$ MEFs were cotransfected with expression vectors for ATF6 and C/EBP-β, and the cells were treated with IFN-γ for the indicated time points. Cells were also transfected with either of the vectors alone or mVenus-mCerulean vector as controls for FRET. For FRET microscopy, cells were fixed with paraformaldehyde and were observed with a Zeiss AxioObserver microscope, using a 1.3 N.A., 40× EC Plan-Neofluar objective lens. CFP and FRET images were captured by using a 455-nm LED illuminator, and YFP images were captured under 505-nm LED illumination. High efficiency sets from Zeiss were used to filter CFP, YFP, and FRET fluorescence before separating vertically and horizontally polarized light with a Dual-view (Optical Insights) (11, 12). Images were collected with a water-cooled Orca-R2 camera

(Hamamatsu) and processed by using Axiovision software (Zeiss). For quantification, the original image containing vertical and horizontal polarizations was split, and the two polarization images were aligned by using Zeiss Axiovision software. Mean intensities for regions of interest were quantified. Corrective g-factors were measured by using a fluorescein solution, and data were analyzed as described (11) by using Microsoft Excel and Graphpad Prism software. Anisotropy images were generated by using Image J software and pseudocolored with the blue/orange ICB look up table. Noncellular regions were masked by using the threshold technique for presentation clarity. Mean intensities for regions of interest were quantified by using the same software. Fluorescence anisotropies for CFP and FRET images were calculated from background subtracted values as described (11).

Indirect and Direct Immunofluoresence. These analyses were conducted as described (13, 14). For indirect immunofluoresence, mouse monoclonal anti-FLAG (1:500), anti-HA (1:200), or anti-LC3 (1:100) were used as primary antibodies and FITC-conjugated anti-mouse IgG (1:50) was the secondary antibody. For direct immunofluoresence, either GFP-LC3 or DS1-GT (Golgi marker) was transfected and processed. Images were captured by using an Olympus fluorescence microscope fitted with a digital camera (QICAM) and processed by QCapture Pro-5.1 (QImaging). Mean intensities for regions of interest were quantified by using the NIH Image J software.

Infection with Bacteria. For in vitro infection, *S. enterica* subsp *enterica* serovar *Typhimurium* strain SL1344 (*S. Typhymurium SL1344*) was used at 10:1 ratio to the MEFs.

Quantification of LC3 Puncta. Autophagy was quantified by counting the percentage of cells showing accumulation of FITC or GFP in dots (FITC-LC3 and GFP-LC3 puncta, of a minimum of 25 cells per preparation in three independent experiments). Cells showing mostly diffuse distribution of FITC or GFP in the cytoplasm and nucleus were considered nonautophagic, whereas cells representing several intense punctuate FITC or GFP aggregates were considered as autophagic and quantified by using the NIH Image J software.

In Vitro Infection Assay. *Salmonella enterica* subsp *enterica* serovar Typhimurium strain SL1344 [(*S.* Typhymurium SL1344) kindly provided by Sharon Tennant, Center for Vaccine Development, University of Maryland Medical School] was grown in 10 mL of LB broth overnight under aerobic conditions at 37 °C. One hundred microliters of the overnight culture was inoculated into 10 mL of fresh LB and incubated at 37 °C with shaking for 3 h until midlog phase. The bacteria was washed and resuspended in PBS to obtain the desired concentration of bacteria. MEFs were infected with *S.* Typhimurium at a MOI of 1:10 (cell:bacteria) for 1 h at 37 °C, 5% CO_2. The cells were further incubated for 30 min in media containing 100 μg/mL gentamycin to remove the extracellular bacteria. The cells were washed three times and fixed in 1% (vol/vol in phosphate buffered solution) formalin. They were then stained with LC3-specific antibody. Treatment with 3-MA was given 1 h before infection with bacteria.

SI Results

RNAi-Mediated Inhibition of ATF6 IFN-Induced Expression of DAPK1. We also used RNAi with shRNAs capable of targeting ATF6 in a mouse- and human-specific manner (see differences in target sequence). MEFs and hTERT-HME1 (a nononcogenic human mammary epithelial cell line) were used for these studies. The shRNAs suppressed the expression of endogenous ATF6 protein in a species-specific manner (Fig. S1 *A* and *B*). IFN-γ induced *DAPK1* mRNA and protein in the controls (empty vector-pLKO-1, and a nontargeting shRNA) but not when ATF6 was knocked down (Fig. S1 *C–F*). In contrast to *Dapk1*, the IFN-γ–induced expression of *Irf1* was unaffected by ATF6-specific shRNAs (Fig. 1 *C* and *D*), indicating an intact STAT1-driven IFN signaling in these cells. Lastly, *Dapk1-Luc* reporter was not induced upon ATF6-knockdown by using RNAi (Fig. S1*G*).

Effect of IFN-γ on the Translocation of Endogenous ATF6. To examine whether endogenous ATF6 similarly translocated to nucleus via Golgi apparatus, we repeated the immunofluorescence analyses in wild-type MEFs by using antibodies that detected ATF6 and the Golgi-specific marker GM-130. ATF6 was primarily found in the perinuclear and cytoplasmic regions compared with the nucleus in steady-state ATF6 (Green fluorescence in Fig. S3*A*). GM130 was detected in Golgi as expected (red fluorescence). IFN-γ treatment for 2 h caused a translocation of ATF6 to the Golgi apparatus, which was consistent with the convergence of red and green signals. Thereafter, Golgi-ATF6 signals declined with a progressive increase in nuclear ATF6 (Cyan fluorescence). By 16 h, a decline and a rise in the nuclear and cytoplasmic ATF6 levels, respectively, were observed. Fig. S3*B* shows the quantified fluorescence signal intensities. Thus, upon IFN treatment, endogenous ATF6 transits through the Golgi before its nuclear entry.

Inhibition of IFN-Induced Autophagy by 3-Methyl Adenine. Because GFP-LC3 is exogenously expressed and may cause certain artifacts some times, we ascertained the IFN-induced autophagic response by performing immunofluorescence analyses with a LC3-specific antibody. Consistent with the observations made with GFP-LC3, we detected higher numbers of LC3 puncta in WT MEFs upon IFN-γ treatment than *Atf6*$^{-/-}$ MEFs (Fig. S5). Treatment with the autophagy inhibitor 3-methyl adenine (3-MA) suppressed the formation of IFN-γ–induced LC3 puncta. Quantified LC3 puncta from multiple fields revealed significant loss of puncta formation in *Atf6*$^{-/-}$ MEFs (Fig. S5, *Right*).

1. Thuerauf DJ, Morrison L, Glembotski CC (2004) Opposing roles for ATF6alpha and ATF6beta in endoplasmic reticulum stress response gene induction. *J Biol Chem* 279: 21078–21084.
2. Yamamoto K, et al. (2007) Transcriptional induction of mammalian ER quality control proteins is mediated by single or combined action of ATF6alpha and XBP1. *Dev Cell* 13:365–376.
3. Zhu C, Johansen FE, Prywes R (1997) Interaction of ATF6 and serum response factor. *Mol Cell Biol* 17:4957–4966.
4. Shen J, Prywes R (2005) ER stress signaling by regulated proteolysis of ATF6. *Methods* 35:382–389.
5. Shen J, Prywes R (2004) Dependence of site-2 protease cleavage of ATF6 on prior site-1 protease digestion is determined by the size of the luminal domain of ATF6. *J Biol Chem* 279:43046–43051.
6. Gade P, Roy SK, Li H, Nallar SC, Kalvakolanu DV (2008) Critical role for transcription factor C/EBP-beta in regulating the expression of death-associated protein kinase 1. *Mol Cell Biol* 28:2528–2548.
7. Kang TJ, et al. (2005) Murine macrophages kill the vegetative form of Bacillus anthracis. *Infect Immun* 73:7495–7501.
8. Furlan-Magaril M, Rincón-Arano H, Recillas-Targa F (2009) Sequential chromatin immunoprecipitation protocol: ChIP-reChIP. *Methods Mol Biol* 543:253–266.
9. Nagai T, et al. (2002) A variant of yellow fluorescent protein with fast and efficient maturation for cell-biological applications. *Nat Biotechnol* 20:87–90.
10. Rizzo MA, Springer GH, Granada B, Piston DW (2004) An improved cyan fluorescent protein variant useful for FRET. *Nat Biotechnol* 22:445–449.
11. Piston DW, Rizzo MA (2008) FRET by fluorescence polarization microscopy. *Methods Cell Biol* 85:415–430.
12. Rizzo MA, Piston DW (2005) High-contrast imaging of fluorescent protein FRET by fluorescence polarization microscopy. *Biophys J* 88:L14–L16.
13. Shen J, Chen X, Hendershot L, Prywes R (2002) ER stress regulation of ATF6 localization by dissociation of BiP/GRP78 binding and unmasking of Golgi localization signals. *Dev Cell* 3:99–111.
14. Vergne I, et al. (2009) Control of autophagy initiation by phosphoinositide 3-phosphatase Jumpy. *EMBO J* 28:2244–2258.

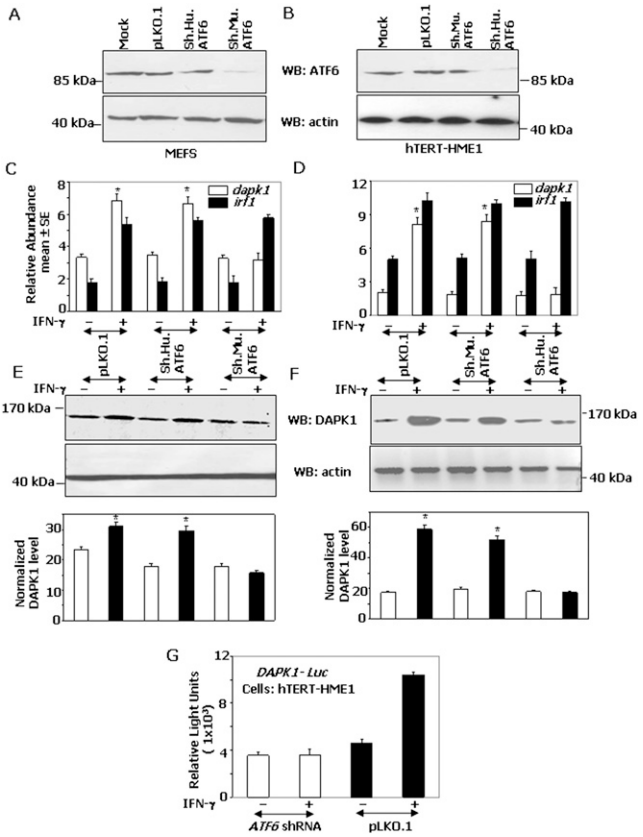

Fig. S1. RNAi-mediated ATF6 knockdown and effect on DAPK1 expression. Western blot analysis of MEFs (*A*) and hTERT-HME1 (*B*) cell lines infected with Lentiviral vectors coding for ATF6-specific shRNAs or the control empty vector (pLKO-1). (*C* and *D*) qPCR analysis of the *Dapk1* and *Irf1* transcripts in MEFs and hTERT-HME1 cells, respectively. Mean ± SE ($n = 6$, $^*P < 0.001$ with respect to control). (*E* and *F*) Western blot analyses of the DAPK1 protein in MEFs and hTERT-HME1 cells, respectively. (*E* and *F Lower*) Respective normalized DAPK1 protein levels. (*G*) Indicated cell type was cotransfected with the *DAPK1-Luc* construct (300 ng) along with a β-*actin*–β-*galactosidase* reporter (100 ng). Luciferase activity was normalized to that of cotransfected β-*actin*–β-*galactosidase* reporter expression. $n = 5$ for each data point.

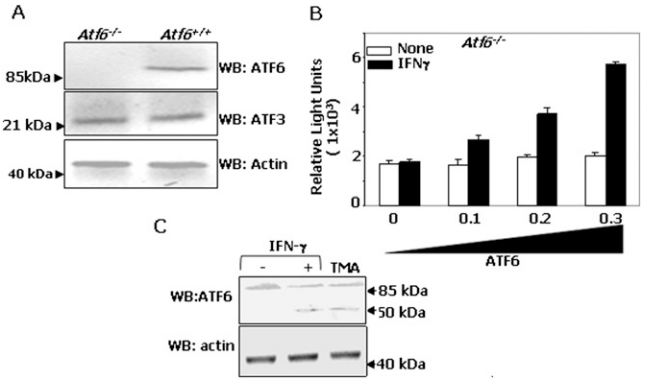

Fig. S2. Validation of *Atf6*$^{-/-}$ MEFs. (*A*) Western blot analyses with the indicated antibodies were performed. (*B*) MEFs were cotransfected with the *Dapk1*-Luc construct (300 ng) along with a β-*actin*–β-*galactosidase* reporter (100 ng) and increasing amounts of ATF6 (0–0.3 μg). In the case of control, 0.3 μg of empty vector was used. Total transfected DNA was kept constant (usually less than 700 ng) by adding vector DNA as required. Luciferase activity was normalized to that of β-galactosidase in each experiment. Each bar represents the mean ± SE ($n = 6$). (*C*) Western blot analyses with the indicated antibodies were performed.

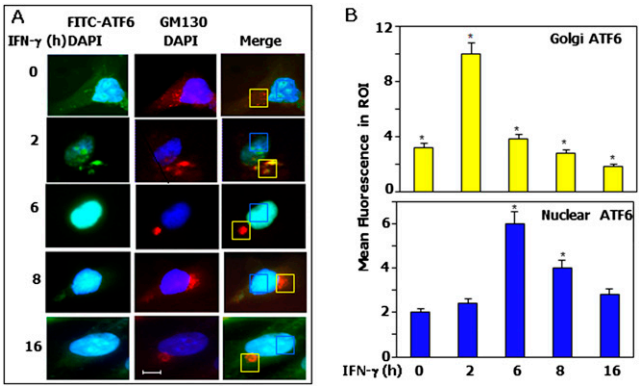

Fig. S3. IFN-γ-induced translocation of endogenous ATF6 into nucleus. (*A*) Immunofluorescence images of DAPI, GM130 (Golgi marker), and FITC (ATF6). (Scale bar: 20 μm.) (*B*) Quantified fluorescence of FITC in ROI. Mean ± SE (n = 10 fields; $^*P < 0.001$).

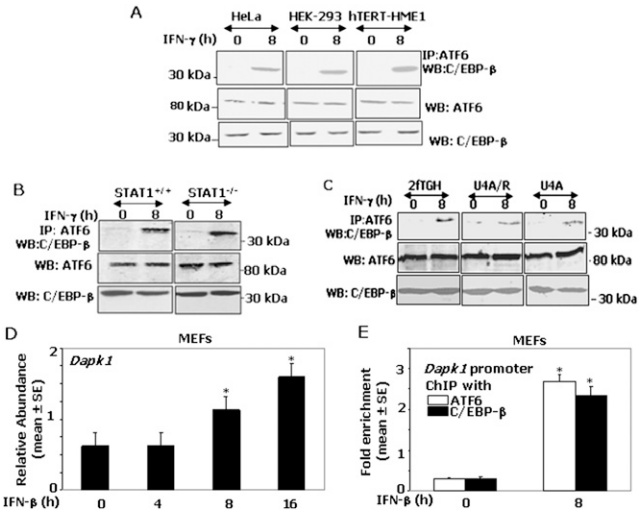

Fig. S4. IFN-γ–stimulated association of C/EBP-β and ATF6 in different cell lines. (*A*–*C*) Indicated cell lines were treated with IFN-γ and were subjected to immunoprecipitation and Western blot analyses. 2fTGH, parent cell line; U4A, JAK1-deficient; U4A/R, JAK1 restored into U4A (1). (*D*) Real-time PCR analysis of IFN-β–induced expression of *Dapk1* transcripts in MEFs cells. Each bar represents the mean ± SE (n = 6, $^*P < 0.01$ with respect to untreated control). (*E*) ChIP assays with the indicated antibodies were performed, and the products were quantified by using qPCR analysis (n = 9 per sample, $^*P < 0.01$ with respect to untreated cotnrol). Input normalized soluble chromatin was used for ChIP assays from each sample.

1. Müller M, et al. (1993) The protein tyrosine kinase JAK1 complements defects in interferon-alpha/beta and -gamma signal transduction. *Nature* 366:129–135.

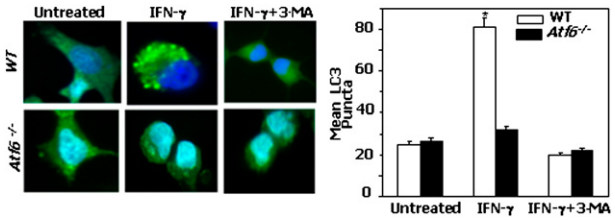

Fig. S5. Formation of IFN-induced LC3 puncta and its inhibition by 3-methyl adenine (3-MA). Endogenous LC3 puncta formation in WT and *Atf6*$^{-/-}$ MEFs. We added 3-MA (5 μM) to the culture 1 h before IFN treatment. LC3 puncta were quantified as above ($^*P < 0.001$, n = 10). The bar graph shows quantified data from multiple fields.

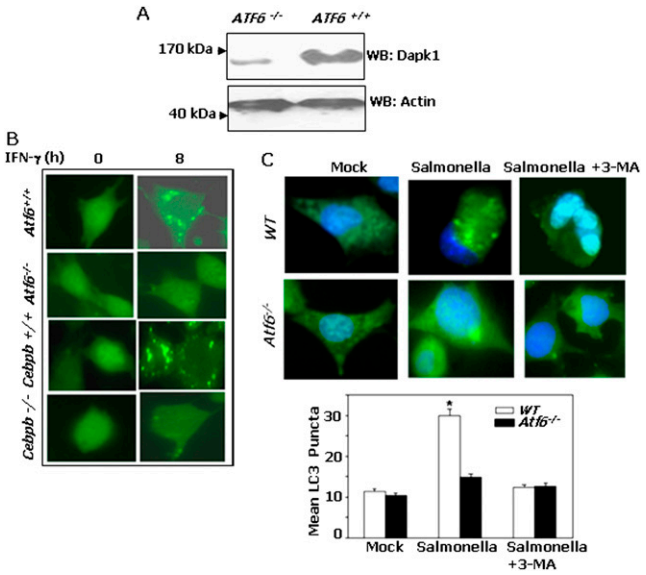

Fig. S6. Analysis of IFN-γ and *Salmonella*-induced LC3 puncta formation. (*A*) Typical Western blot analysis with indicated antibodies in specific cell types was shown. (*B*) $Atf6^{+/+}$, $Atf6^{-/-}$, $Cebpb^{+/+}$, and $Cebpb^{-/-}$ MEFs stably transfected with GFP-LC3 and were treated as indicated. LC3 puncta in the indicated cell types were shown. (C) Endogenous LC3 puncta formation in *WT* and $Atf6^{-/-}$ MEFs in vitro infection assay with *Salmonella*. (*C Lower*) LC3 puncta quantification (n = 10 fields) from three independent experiments ± SD. *$P < 0.01$ with respect to $Atf6^{-/-}$ MEFs.